

Neutrino Oscillations in the Project-X Era

M. Bishai, M.V. Diwan, J. Stewart, B. Viren, E. Worcester
Physics Department, Brookhaven National Laboratory, Upton, NY 11973

Lisa Whitehead
Physics Department, University of Houston, Houston, TX

Geralyn Zeller
Particle Physics Division, Fermi National Accelerator Laboratory, Batavia, IL

(Dated: January 4, 2012)

Abstract

If the recent indications of a modest size for the mixing angle θ_{13} persist then the science of neutrino oscillations will shift to precision determination of the CP phase and explicit demonstration of CP violation. Any additional contributions from new physics to the oscillation channel $\nu_\mu \rightarrow \nu_e$ could be uncovered by multiple constraints in the $(\theta_{13}, \delta_{CP})$ parameter space. In long baseline experiments such constraints will require examination of the oscillation strength at higher L/E where the effects of CP violation will be large. For the fixed baseline of 1300 km for LBNE (Fermilab to Homestake), it will be important to examine oscillations at low energies (< 1.5 GeV) with good statistics, low backgrounds, and excellent energy resolution. The accelerator upgrades in the Project-X era have the potential to offer the beams of the needed intensity and quality for this advanced science program. In this note we examine the event rates for high intensity low energy running of Project-X and the Fermilab Main Injector complex, and the precision in the $(\theta_{13}, \delta_{CP})$ space.

We find that the best way to obtain multiple constraints in the neutrino sector is to perform high statistics experiments with low energy neutrino beams over long distances. For oscillation physics at low energies the charged current cross section is dominated by quasielastic scattering. For the quasielastic final state any large detector capable of measuring single lepton final states is adequate, however the water Cherenkov detector is the only one that can achieve the needed target mass (~ 200 kTon) to obtain the needed statistical precision.

I. INTRODUCTION

Recent indications of a modest size for the third mixing angle (θ_{13}) in the neutrino sector allow us to plan for the future program of precision neutrino physics. If these indications continue to hold ($\sin^2 2\theta_{13} \sim 0.1$), then a rich new system will become available for the physics of neutrino oscillations, and leptonic CP violation.

Once the parameters of neutrino mixing have been measured it will be necessary to exploit the new system to find indications of departures from the Standard Model with massive neutrinos (ν SM). These departures could come from additional low energy interactions or unexpected mixing. It is not possible to predict the exact nature of new physics or investigate every model for new neutrino physics that is now being discussed in the theoretical literature. Nevertheless, it is possible to sketch some generic attributes regarding the design of a new experiment that is likely to yield indications of new physics. These necessary attributes would be based on physics that is known, physics that has already been excluded, and reasonable extrapolations of scientific strategies that have worked in the past.

The science of neutrino oscillations is a low energy phenomena at the achievable baselines. Moreover most of the precision measurements in neutrino physics have been performed at low energies. Experiments that have yielded the best results are at high $L/E \gg 500 \text{ km/GeV}$, or for any fixed distance, the lowest energy neutrinos have provided the best science. This is demonstrated in figure 1. Experiments designed for high energy operation probe mixing in the region of $\Delta m^2 > 1 \text{ eV}^2$. Previous results as well as the direct limits on neutrino mass from tritium beta decay ($m_{\nu_e} < 2 \text{ eV}$ at 95% C.L.) and astrophysics ($\sum_i m_{\nu_i} < 0.4 - 1 \text{ eV}$) have put severe limits on physics at $L/E < 1 \text{ km/GeV}$ [1]. Furthermore, any remaining issues such as the LSND/MiniBoone/reactor anomalies are best resolved by short baseline experiments.

In the following, we first calculate the oscillation probability for $\nu_\mu \rightarrow \nu_e$ as a function of energy using the best values for the oscillation parameters. We will then calculate the energy spectrum of neutrinos that could be produced by various beams from Fermilab. Finally we calculate the precision in the $(\theta_{13}, \delta_{CP})$ space for an example running condition, and comment on constraints on other parameters that could result from the data.

For oscillation physics at low energies the charged current cross section is dominated by quasielastic scattering as shown in figure 2. For the quasielastic final state any large detector capable of measuring single lepton final states is adequate, however the water Cherenkov detector is the only one that can achieve the target mass needed to obtain the statistical precision. In the following we will therefore assume a 200 kTon fiducial water Cherenkov detector for the target mass.

II. $\nu_\mu \rightarrow \nu_e$ OSCILLATIONS

The oscillation mode with the richest scientific content is the appearance mode $\nu_\mu \rightarrow \nu_e$ (or $\nu_e \rightarrow \nu_\mu$) and its anti-neutrino counterpart. The oscillation strength for this mode as a function of distance and energy contains contributions from all parameters of the neutrino mixing matrix and all three neutrino mass eigenstates.

Assuming a constant matter density, the oscillation of $\nu_\mu \rightarrow \nu_e$ in the Earth for 3-generation mixing is described approximately by the following equation [2]

$$\begin{aligned}
 P(\nu_\mu \rightarrow \nu_e) \approx & \sin^2 \theta_{23} \frac{\sin^2 2\theta_{13}}{(\hat{A} - 1)^2} \sin^2((\hat{A} - 1)\Delta) \\
 & + \alpha \frac{\sin \delta_{CP} \cos \theta_{13} \sin 2\theta_{12} \sin 2\theta_{13} \sin 2\theta_{23}}{\hat{A}(1 - \hat{A})} \sin(\Delta) \sin(\hat{A}\Delta) \sin((1 - \hat{A})\Delta) \\
 & + \alpha \frac{\cos \delta_{CP} \cos \theta_{13} \sin 2\theta_{12} \sin 2\theta_{13} \sin 2\theta_{23}}{\hat{A}(1 - \hat{A})} \cos(\Delta) \sin(\hat{A}\Delta) \sin((1 - \hat{A})\Delta)
 \end{aligned}$$

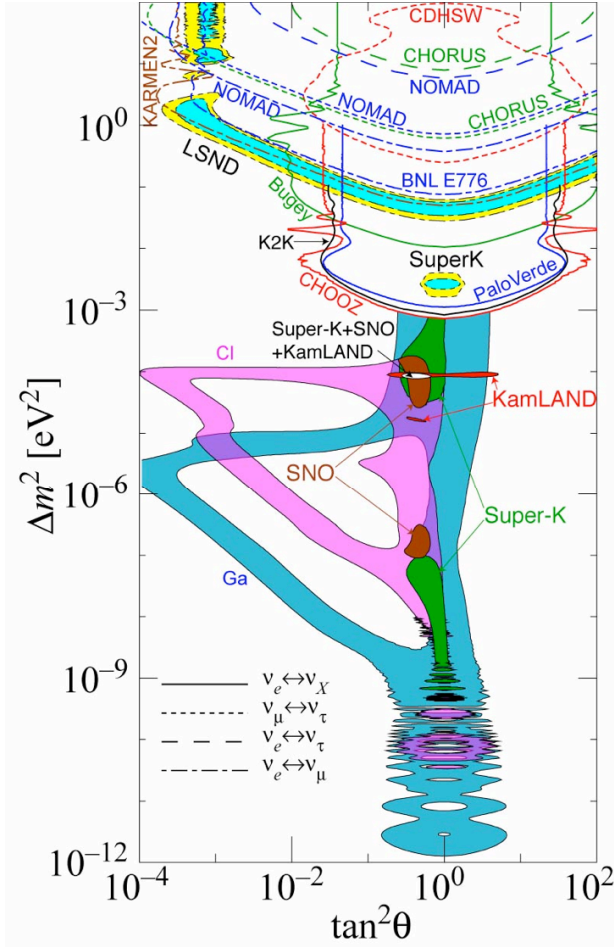


FIG. 1: Compilation of neutrino oscillation limits and results. The filled areas are positive indications and lines correspond to 90% confidence level limits unless otherwise indicated. Source: <http://hitoshi.berkeley.edu>

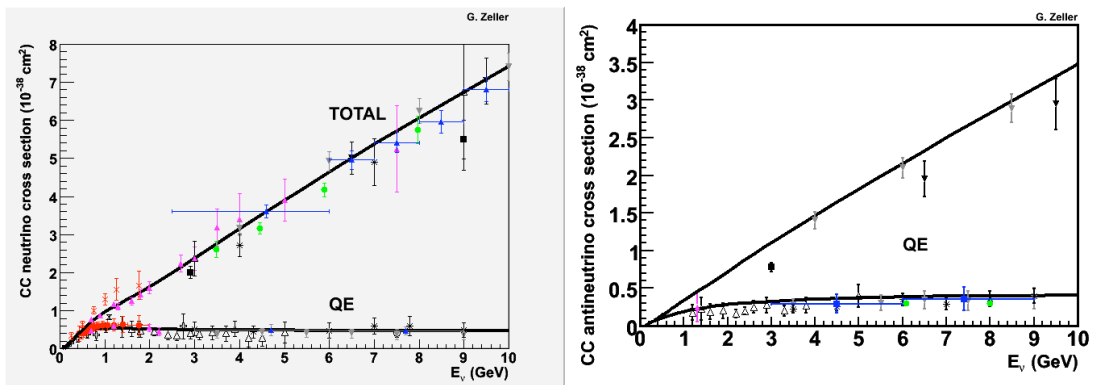


FIG. 2: Charged current neutrino total cross section as a function of energy for neutrinos (left) and antineutrinos (right). The cross section of quasielastic interactions is also displayed. The error bars are the data and the lines are the current best model. It should be noted that below 1.5 GeV the total cross section is dominated by quasielastic interactions. Source: G. Zeller.

$$+\alpha^2 \frac{\cos^2 \theta_{23} \sin^2 2\theta_{12}}{\hat{A}^2} \sin^2(\hat{A}\Delta) \quad (1)$$

where $\alpha = \Delta m_{21}^2 / \Delta m_{31}^2$, $\Delta = \Delta m_{31}^2 L / 4E$, $\hat{A} = 2VE / \Delta m_{31}^2$, $V = \sqrt{2}G_F n_e$. n_e is the density of electrons in the Earth. Recall that $\Delta m_{31}^2 = \Delta m_{32}^2 + \Delta m_{21}^2$. Also notice that $\hat{A}\Delta = LG_F n_e / \sqrt{2}$ is sensitive to the sign of Δm_{31}^2 . For anti-neutrinos, the second term in Equation 1 has the opposite sign. It is proportional to the following CP violating quantity.

$$J_{CP} \equiv \sin \theta_{12} \sin \theta_{23} \sin \theta_{13} \cos \theta_{12} \cos \theta_{23} \cos^2 \theta_{13} \sin \delta_{CP} \quad (2)$$

Equation 1 is an expansion in powers of α . This approximate formula is useful for understanding important features of the appearance probability: 1) the first three terms in the equation control the matter induced enhancement for normal mass ordering ($m_1 < m_2 < m_3$) or suppression for the reversed mass ordering ($m_3 < m_1 < m_2$) of the oscillation probability above 3 GeV; 2) the second and third terms control the sensitivity to CP in the ~ 1 GeV range; and 3) the last term controls the sensitivity to Δm_{21}^2 at low energies. The last term is also proportional $\cos^2 \theta_{23}$, and therefore is sensitive to the issue of maximum mixing in $\theta_{23} = \pi/4$. As previously explained [3], measurement of the spectrum of oscillated ν_e events will allow us access to all of these parameters in a single experiment with good control of systematics.

The oscillation probability for $\nu_\mu \rightarrow \nu_e$ for both neutrino and anti-neutrino modes and for normal and reversed mass ordering is plotted in figure 3 using current best known parameters including the value $\sin^2 2\theta_{13} = 0.1$ [4]. It is easy to see that the oscillation probability will be in the 5-10 % range at the first oscillation maximum between 2 - 3 GeV, but at lower energies both the size of the probability and the effect of the CP phase will be dramatic. The lower energy oscillation effect is also relatively less affected by the mass hierarchy. A measurement of these probabilities across the energy range will certainly result in precise new information about the mechanism of neutrino oscillations.

III. EVENT RATES FOR LBNE FOR VARIOUS PROJECT-X BEAM CONDITIONS

The relevant energy range of oscillations over 1300 km can be seen from figure 1 to be from 0.2 GeV to 4 GeV. Any flux above 4 GeV is not going to contribute much to physics, and events below 0.2 GeV will most likely have poor resolution. Neutrinos in the 0.2 to 4 GeV energy range are produced by pions of energy $\sim 0.5 - 10$ GeV. We shall assume that the proton energy available from Project-X and related upgrades will be in the 8 to 120 GeV range. The production spectrum of neutrinos in the laboratory frame is affected by the proton energy, the focusing efficiency of the target/horn system, and finally the kinematics of pion decay. In the center of mass of proton collisions, pion production is distributed in an approximate normal distribution as a function of rapidity and increases only logarithmically as a function of $\sqrt{s} \propto \sqrt{E_{protons}}$. In the laboratory frame this distribution of pions is boosted by a factor $\gamma_{cm} \sim \sqrt{E_{proton}}$. For higher proton energies, there are higher number of pions produced at high rapidity in the center of mass, and they are boosted to higher energies in the laboratory frame. Both effects are such that in our proton and pion energy range, the production of pions at any given energy is roughly proportional to the energy of the protons and, obviously, the total current of protons, or the total proton beam power. If we assume that the target/horn system can be tuned to focus pions efficiently at any energy above 0.5 GeV, the neutrino yield is further affected by the kinematics of pion decay. The flux of neutrinos from pion decay in the forward region is proportional to $\gamma_\pi^2 \propto E_\pi^2$. The two kinematic effects – the production of pions as a function of proton energy and the pion decay kinematics – are such that the only way to boost the yield of neutrinos at low energies is with high proton beam power at low energies.

In table I we have made a list of beam conditions that could be possible from Project-X and the Project-X upgrade at 8 GeV. Figure 4 shows the beam power available from the Main Injector as a

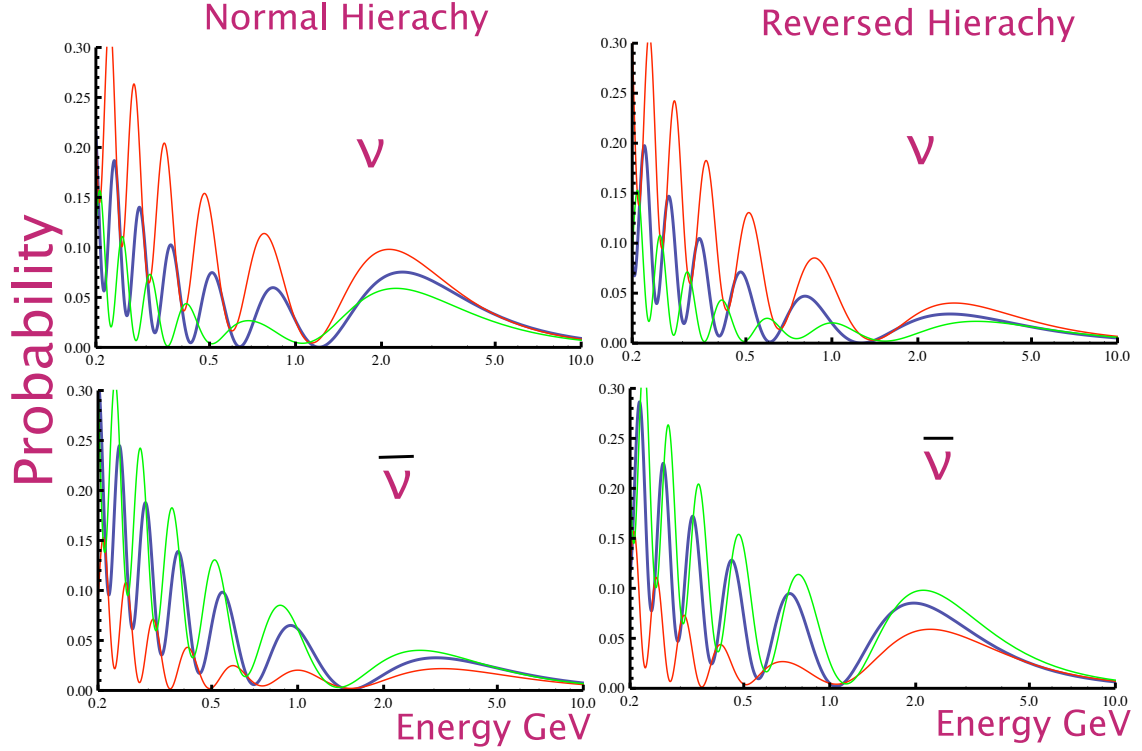


FIG. 3: Appearance probability for $\nu_\mu \rightarrow \nu_e$ as a function of energy at a distance of 1300 km. The top plots are for neutrinos and bottom plots are for anti-neutrinos. The left side plots are for normal mass ordering and right hand side are for reversed mass ordering. The parameters used for these plots are $\Delta m_{32}^2 = 0.0025eV^2$, $\Delta m_{12}^2 = 7.6 \times 10^{-5}eV^2$, $\theta_{23} = \pi/4$, $\theta_{12} = 34^\circ$, $\theta_{13} = 9.2^\circ$. The blue curve in all cases is for $\delta_{CP} = 0$ and the red and green curves are for $\delta_{CP} = \pi/2$ and $-\pi/2$, respectively.

function of energy. With Project-X the beam power from the Main Injector can be maintained at or above 2 MW over the range 60 - 120 GeV. This is because the decrease in energy can be (mostly) compensated by increasing the repetition rate. This trend continues as the energy decreases but at some point it is limited by the number of protons coming from the LINAC. The power achievable at 30 GeV would be ~ 1.3 MW for the Project-X Reference Design. The Main Injector requires 270 kW of incident 8 GeV beam power at 8 GeV to produce ~ 2 MW at 60 GeV. With the additional upgrade to the 8 GeV pulsed LINAC, the 8 GeV power level could be increased to ~ 4 MW. In such a scenario, the Fermilab accelerator complex could produce multi-MW power at both 60 GeV and 8 GeV simultaneously. The duty factor for any Main Injector operation would continue to remain small in the single turn extraction mode, however the duty factor at 8 GeV will be $\sim 5 - 10\%$ unless a ring is deployed to compress the beam further. The poor duty factor is not problematic as long as the far detector is deployed at depth.

For our calculations of event rates and neutrino spectra, we will use operation at 60 GeV at 2 MW and operation at 8 GeV at 3 MW. We have calculated the beam spectra using a GEANT4 simulation of the LBNE beamline with magnetic horns with a current of 250 kAmps, 2 meter diameter decay tunnel with a length of 280 meters. The LBNE beamline was designed for high energy operation. There is currently no design to transport 8 GeV protons to the LBNE target. The 8 GeV beam will require either another beamline or substantial modifications to the current beamline. Here we will not investigate these important technical issues regarding the beamline, but we recognize that simultaneous operation at 8 and 60 GeV is quite compelling and should be investigated. In the following we focus on the neutrino spectra and event rates.

The muon neutrino and antineutrino spectra (without oscillations) for 8 GeV and 60 GeV beams are shown in figure 5 superimposed on the expected $\nu_\mu \rightarrow \nu_e$ oscillation probability. The event

Accelerator Stage	Energy	Current	Duty Factor	Power
CW LINAC	3 GeV	1 mA	CW	2870 kW
Pulsed LINAC	8 GeV	40 μ A	4.4ms/0.1sec	350 kW
8 GeV Upgrade	8 GeV	460 μ A	6.7ms/0.07sec	4270 kW
Main Injector	60 GeV	37 μ A	9.5 μ S/0.7sec	2020 kW
Main Injector	120 GeV	20 μ A	9.5 μ S/1.3sec	2200 kW

TABLE I: Beam conditions and power possible during the Project-X phase. An accumulator ring at 8 GeV could be used to improve the duty factor. Source: Tschirhart

rate is calculated for the total muon neutrino (and antineutrino) cross section shown in figure 2. The two different energy spectra are shown to complement each other. The 8 GeV spectrum covers the low energy region where large CP phase effects exist while the 60 GeV spectrum covers the higher energy region where the matter effects will dominate. It should be remarked that the 60 GeV beam also has similar numbers of events at low energies as the low energy beam, but the low energy beam is expected to have somewhat more rate and less backgrounds due to event mis-reconstruction. The beam contamination in these beams is shown in table II where the total event rate is tabulated for each component of the beam. The event rate after ν_μ disappearance is also shown for the muon neutrino component. A few comments are in order regarding this table:

- The event rates have been calculated for the total cross section as in figure 2. In the next section we will use the tabulated water Cherenkov detector performance for extracting electron neutrino events and associated backgrounds.
- The 60 GeV beam is very well tuned for the first oscillation maximum and consequently has a large effect due to muon neutrino disappearance. Almost 75% of the total muon neutrino events are calculated to disappear. This factor is smaller for the 8 GeV beam because of multiple oscillation nodes.
- The neutrino contamination in the antineutrino beam is large $\sim 26\%$ for the 60 GeV beam, but it is much smaller for the 8 GeV beam. Nevertheless, the event rate for the antineutrino running in the 8 GeV beam is much more suppressed compared to the neutrino running. This difference can be traced back to both the production rate of π^- and the neutrino/antineutrino cross sections at low energies. The large suppression of anti-neutrino rates at low energies is the additional reason for the complementarity between high and low energy running for LBNE.

IV. ELECTRON NEUTRINO APPEARANCE AND PRECISION CP VIOLATION MEASUREMENTS

We have tabulated the performance of the water Cherenkov detector using data analysis from Super-Kamiokande (SK). This performance has been verified by several independent checks on SK data. The performance of the 200 kTon LBNE water detector is expected to be similar or better because of higher pixelation and much better time resolution of the photo-multiplier tubes. Work

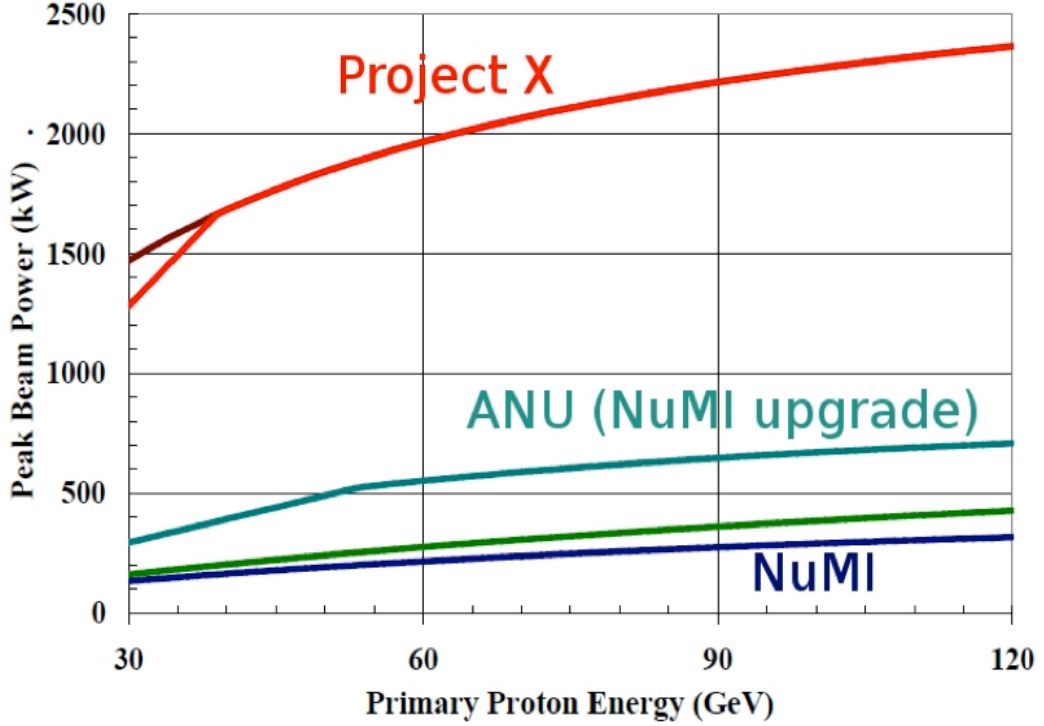


FIG. 4: Proton beam power as a function of proton energy from the Fermilab Main Injector. Shown are current capabilities labeled as NuMI. The recently funded upgrades (labeled as ANU) will increase the power to 550 kW at 60 GeV or 700 kW at 120 GeV. Project-X as currently conceived will allow beam power of 2 MW at 60 GeV and 2.3 MW at 120 GeV.

Event type	8 GeV	60 GeV	8 GeV	60 GeV
	ν	ν	$\bar{\nu}$	$\bar{\nu}$
$\nu_{\mu}CC$	8900	66000	200	5870
w/osc	4600	17100	101	2900
$\bar{\nu}_{\mu}CC$	76	1800	1900	22000
w/osc	36	850	1030	5800
ν_eCC	95	580	1	69
$\bar{\nu}_eCC$	1	14	23	172

TABLE II: Total rate of events for the 8 GeV and 60 GeV neutrino and antineutrino beams. The 8 GeV (60 GeV) beam is assumed to have power of 3 MW (2MW). The running time is one year and the detector fiducial mass is 200 kTon at 1300 km from Fermilab. The event rate after the disappearance of muon neutrinos by oscillations is also shown for the muon neutrino and antineutrino components.

continues to fully simulate and reconstruct events in the 200 kTon water Cherenkov detector. A recent eye-scan of the Monte Carlo events indicates considerable room for improvement beyond the Super-Kamiokande based performance by including low multiplicity events. Nevertheless, in the following we have used the SK based signal efficiency and background rejection since it is the most conservative estimate.

The calculation is performed by first using the total charged current and neutral current event

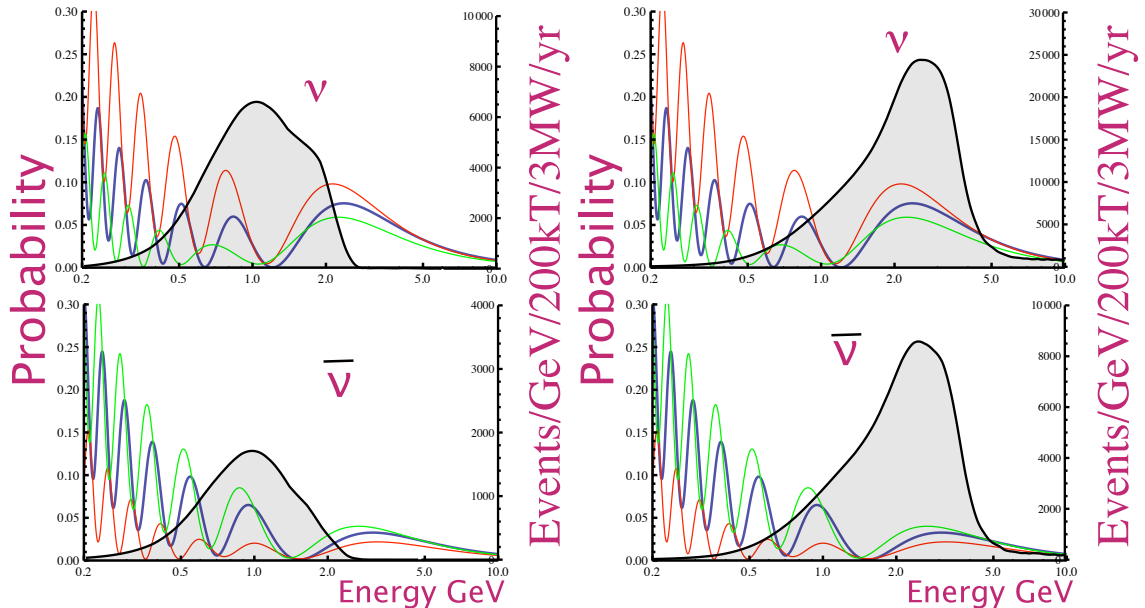


FIG. 5: Spectra of event rates as a function of energy for 8 GeV (left) and 60 GeV (right) proton beams from Fermilab. The spectra are superimposed on the expected oscillation probability for normal hierarchy. Spectra are for the total charged current cross-section for muon neutrino (top) and antineutrinos (bottom). The beam is from Fermilab to Homestake over a distance of 1300 km; the intensity for the 8 GeV beam is assumed to be 3 MW and for 60 GeV it is 2 MW. The detector size is 200 kTon fiducial mass.

spectrum as a function of neutrino energy and using the efficiency for selecting events reconstructed as single electromagnetic showers with no signatures of additional particles including decays of muons that might be below Cherenkov threshold. This calculation includes the expected energy resolution and smearing of both charged current and neutral current events. After obtaining the spectrum of these events using tabulated efficiency factors, we use a tabulated event identification likelihood efficiency (LL) as a function of *reconstructed* energy. This likelihood performance was also tabulated using SuperK Monte Carlo that has been tuned to atmospheric neutrino data. The likelihood performance tabulation includes the efficiency for charged current electron neutrino signal events and both neutral current and charged current muon neutrino events. The likelihood performance can be tuned to obtain high signal efficiency (for example, from 80%LL to 40%LL) and different levels of background rejection.

We have used the parameterized performance for the water detector using the 60 GeV and 8 GeV beams to calculate the reconstructed spectra with the proper resolution and efficiencies in figures 6 and 7. For the 60 GeV running we have used a likelihood performance that has 40% efficiency for signal in figure 6. The lower efficiency cut reduces the neutral current background above 2 GeV to be approximately the same as the beam contamination of electron neutrinos and provides a spectrum with a large signal to background ratio for both neutrino and anti-neutrino running.

For the 8 GeV running we have used a likelihood performance that has 80% efficiency for signal in figure 7. Such a choice uses the advantages of running a low energy beam which will have lower backgrounds from both the neutral currents and the beam contamination. The advantages of the lower energy beam can be clearly seen in the large CP effects below 1 GeV. The appearance signal is seen to vary by more than a factor of 2 over the range $\delta_{CP} = -\pi/2 \rightarrow \pi/2$. It is clear that for the 8 GeV beam, the anti-neutrino event rate will be low. The principle reason for the low rate is the anti-neutrino charge current cross section at low energies. In particular, the quasi-elastic cross section for anti-neutrinos reduces much more rapidly at low energies than for neutrinos. The second reason is the lower production of π^- mesons by lower energy protons. It should also be noted that the large CP effects below 1 GeV are only weakly affected by mass hierarchy.

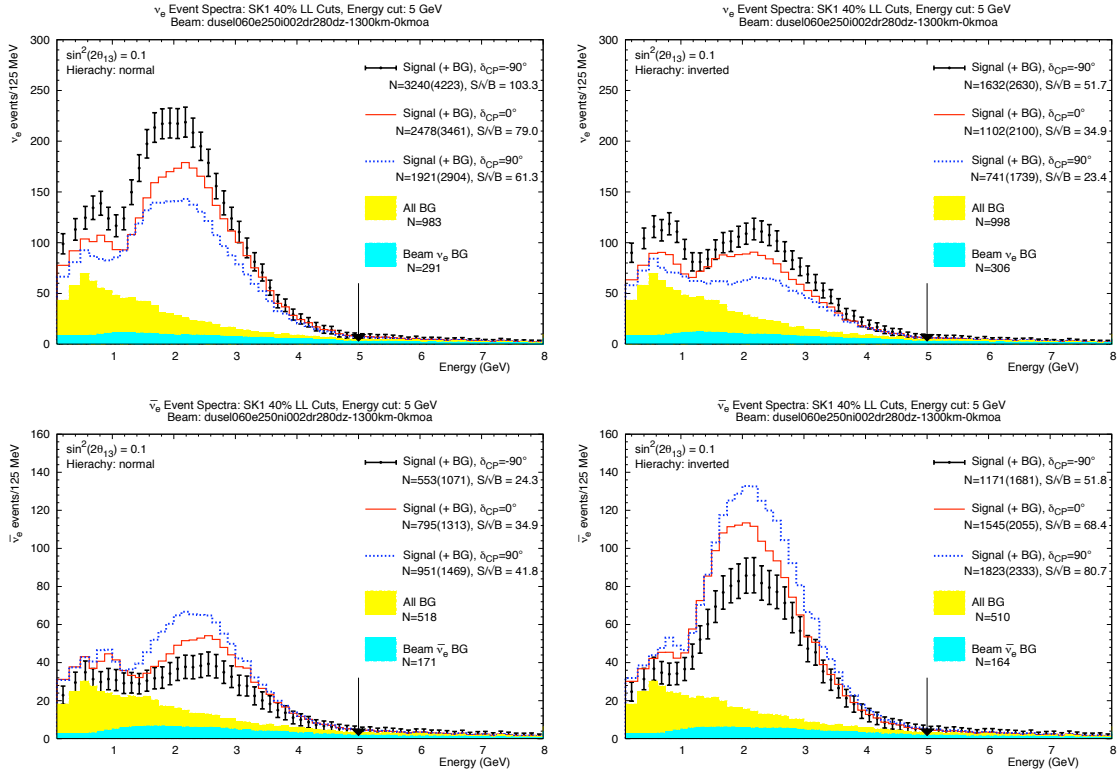


FIG. 6: Event spectra using a 200 kTon water Cherenkov detector at Homestake for a neutrino beam from FNAL. We have assumed 2 MW of power at 60 GeV for 5 years of running for neutrinos (top plots) and antineutrino modes (bottom plots). The left plots are for normal mass hierarchy and right plots are for inverted mass hierarchy. The value for $\sin^2 2\theta_{13} = 0.1$. The curve with error bars in each plot is for $\delta_{CP} = -\pi/2$ and the red and blue curves are for $\delta_{CP} = 0, \pi/2$, respectively. The integral numbers of events are shown in the legends. The integral was computed upto the arrow in the figure.

A simultaneous run of beams at 60 GeV and 8 GeV will provide excellent coverage of appearance spectra across the entire energy region. Moreover, the beam running could be managed in such a way that the two beams provide opposite polarity beams. For example, the 8 GeV beam could run in the neutrino mode and the 60 GeV beam could run in the antineutrino mode. In the case of inverted hierarchy, such a mode of running could be extremely beneficial.

We have used the spectra shown in figures 6 and 7 to calculate the precision with which $\sin^2 2\theta_{13}, \delta_{CP}$ could be measured. These calculations were performed using the GLOBES software program [5]. The precision is shown in figures 8 and 9. For this plot we have used a total of 5 yrs of running in 60 GeV and in 8 GeV beams (as remarked earlier this could be simultaneous). The 60 GeV running is split in neutrino and anti-neutrino modes, but the 8 GeV running is in only the neutrino mode. We will remark on a few features of this measurement:

- The two beams cover very different energy regions and have independent sensitivity. The 60 GeV data will be affected by large matter effects and will result in the resolution of the mass hierarchy with very high ($> 15\sigma$) confidence. Once the mass hierarchy is known, the same data can be used for additional constraints on the matter potential or other contributions to the oscillation as described below.
- The 60 GeV data provides high precision on $\sin^2 2\theta_{13}$ (\sim few percent). The 8 GeV data with neutrino only running will have high precision to δ_{CP} , but it will be correlated to θ_{13} . When

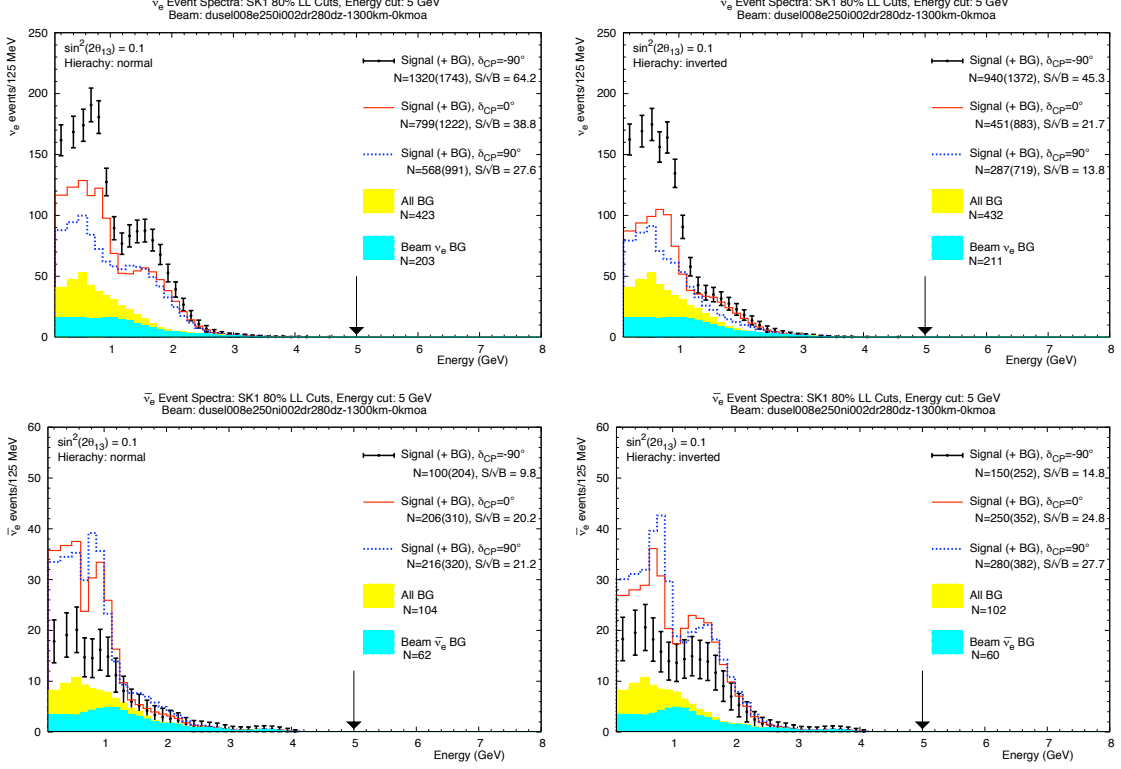


FIG. 7: Event spectra using a 200 kTon water Cherenkov detector at Homestake for a neutrino beam from FNAL. We have assumed 3 MW of power at 8 GeV for 5 years of running for neutrinos (top plots) and antineutrino modes (bottom plots). The left plots are for normal mass hierarchy and right plots are for inverted mass hierarchy. The value for $\sin^2 2\theta_{13} = 0.1$. The curve with error bars in each plot is for $\delta_{CP} = -\pi/2$ and the red and blue curves are for $\delta_{CP} = 0, \pi/2$, respectively. The integral numbers of events are shown in the legends. The integral was computed upto the arrow in the figure.

the two sets of data are combined, a measurement of δ_{CP} with an error of $\pm 10^\circ$ ($\pm 5^\circ$) at $\delta_{CP} = \pi/2$ ($\delta_{CP} = 0$) is possible.

- The two independent data sets form independent constraints on the neutrino oscillation parameters. If there is any additional potential difference between the two mass eigenstates due to new physics it will become evident as a shift in the measured parameters from these two datasets at different energies. Such a shift could appear even if there is no explicit CP violation in the 3-generation picture as represented by the parameter δ_{CP} . This measurement precision could be used as a model independent parameter to test for new physics.
- All calculations of sensitivity so far have assumed that the true value for $\sin^2 2\theta_{23} = 1.0$ or $\theta_{23} = \pi/4$. However, θ_{23} is actually not very well known. The measurement ranges from 35.7° to 53.2° at 3σ . In particular, the value could be above or below 45° . The deviation of θ_{23} from maximum mixing is of high interest to GUT theorist who can predict this particular mixing angle through various models. The deviation of θ_{23} from 45° is indicative of the relationship between quark and lepton mixing.

Our current calculations include a precise determination of $\sin^2 2\theta_{23}$ using the disappearance data from LBNE. This internal constraint is included in the sensitivities published for LBNE. However, the disappearance data is not sensitive to the octant of θ_{23} . The appearance data has excellent sensitivity to the angle θ_{23} as shown in equation 1. The first term of the probability depends on $\sin^2 \theta_{23}$. This can be seen in figure 10. The oscillation probability at

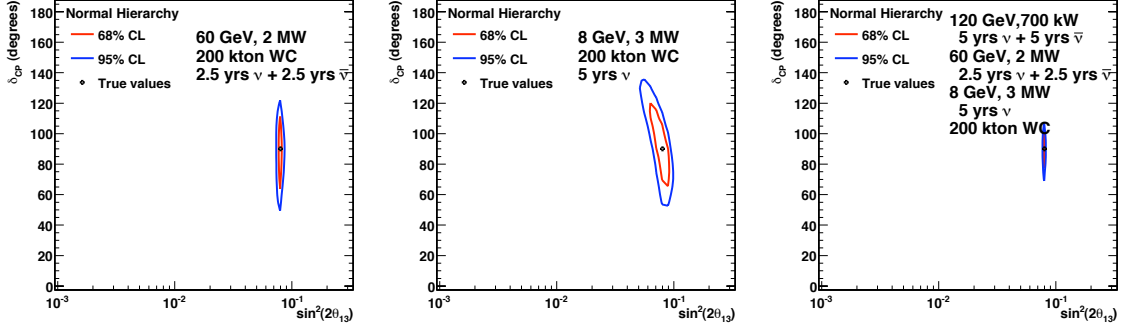


FIG. 8: 2 sigma and 1 sigma confidence level measurements of $\sin^2 2\theta_{13}, \delta_{CP}$ with different running conditions. Left-most plot is for running 60 GeV beam for 2.5 yrs each in neutrino and antineutrino modes. Middle plot is for running the 8 GeV beam only in the neutrino mode for 5 years. The right-most plot is the combination of both running conditions. For this calculation we have assumed $\sin^2 2\theta_{13} = 0.08, \delta_{CP} = \pi/2$ and normal mass ordering.

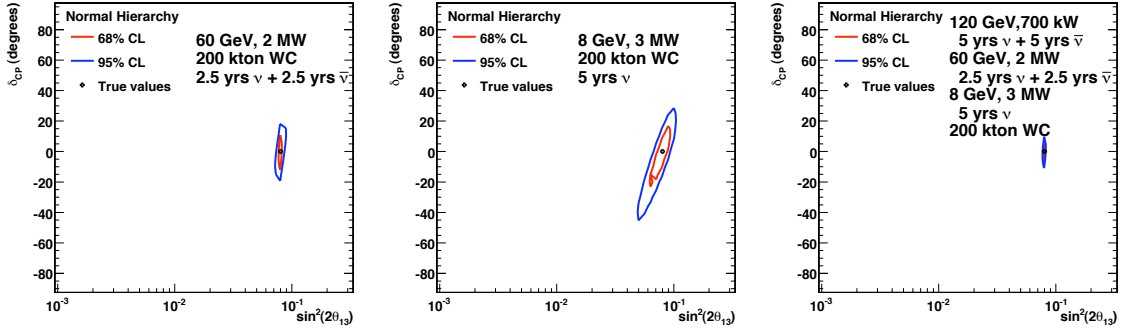


FIG. 9: 2 sigma and 1 sigma confidence level measurements of $\sin^2 2\theta_{13}, \delta_{CP}$ with different running conditions. Left-most plot is for running 60 GeV beam for 2.5 yrs each in neutrino and antineutrino modes. Middle plot is for running the 8 GeV beam only in the neutrino mode for 5 years. The right-most plot is the combination of both running conditions. For this calculation we have assumed $\sin^2 2\theta_{13} = 0.08, \delta_{CP} = 0$ and normal mass ordering.

high energies using the 60 GeV beam is seen to have a large dependence on θ_{23} , but the 8 GeV spectra do not display the same sensitivity. A joint fit using 8 GeV and 60 GeV data is expected to resolve the octant of θ_{23} . We will display this calculation in an update to this note.

Conclusion

We have examined a method to obtain multiple constraints in the neutrino oscillation sector using Project-X with high statistics, low energy neutrinos over long distances. This is motivated by the recent indications of a modest value for $\theta_{13} \sim 9^\circ$. For oscillation physics at low energies the charged current cross section is dominated by quasielastic scattering. For the quasielastic final state any detector capable of measuring single lepton final states is adequate, however the water Cherenkov detector is the only one that can achieve the needed target mass to obtain the statistical

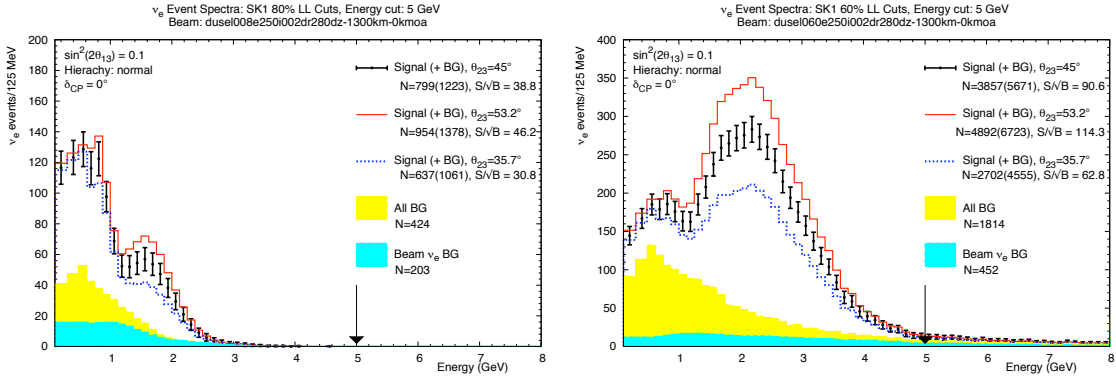


FIG. 10: Effect of θ_{23} variation on the appearance spectra from 8 GeV running (left) and 60 GeV running (right). The integral numbers of events are shown in the legends. The integral was computed upto the arrow in the figure.

precision. And therefore we have used a 200 kTon detector to obtain event spectra and sensitivity in the $(\theta_{13}, \delta_{CP})$ space.

Project-X will allow great flexibility in proton beam energy and power that can be delivered for neutrino beams. In particular, we find the possibility of an upgrade to the pulsed LINAC for Project-X to deliver high power at 8 GeV very interesting. With such an upgrade high power 8 GeV running can be simultaneous with 60 GeV running because only 266 kW of the 8 GeV beam will be fed to the Main Injector to make 2 MW of 60 GeV. The rest of the almost 4 MW of 8 GeV could be used separately for low energy neutrino production. A combination of 8 GeV and 60 GeV running will allow coverage of multiple oscillation nodes with high statistics.

The combined data set from 8 GeV and 60 GeV running will allow multiple independent constraints on the mixing parameters. The shift in the θ_{13}, δ_{CP} solutions from these data sets could be used as a model independent parameter to test for new physics. If the data sets match, very high precision ranging from $\pm 5^\circ$ to $\pm 10^\circ$ on δ_{CP} is possible with a few years of running.

-
- [1] PDG, Review of Particle Physics, Journal of Physics G, Vol. 33, July 2006.
 - [2] M. Freund, Phys.Rev. D64 (2001) 053003; M. Freund, P. Huber, M. Lindner, Nucl.Phys. B615 (2001) 331-357;
 - [3] The study report, all associated documents, presentations, plots, studies, spectra, are at <http://nwg.phy.bnl.gov/fnal-bnl>, Fermilab-0801-AD-E, BNL-77973-2007-IR, arxiv:0705.4396.
 - [4] G. L. Fogli, E. Lisi, A. Marrone, A. Palazzo, A. M. Rotunno, arXiv:1106.6028.
 - [5] P. Huber, M. Lindner and W. Winter Simulation of long-baseline neutrino oscillation experiments with GLOBES arXiv: hep-ph/0407333. P. Huber, J. Kopp, M. Lindner, M. Rolinec and W. Winter New features in the simulation of neutrino oscillation experiments with GLOBES 3.0 arXiv: hep-ph/0701187